VOLUME 112, NUMBER 18
AUGUST 29, 1990


JOURNAL
OF THE
AMERICAN
CHEMICAL
SOCIETY

# Anion Binding to Uteroferrin. Evidence for Phosphate Coordination to the Iron(III) Ion of the Dinuclear Active Site and Interaction with the Hydroxo Bridge

**Shelia S. David and Lawrence Que, Jr.***

*Contribution from the Department of Chemistry, University of Minnesota, 207 Pleasant Street Southeast, Minneapolis, Minnesota 55455.* *Received October 25, 1989*

**Abstract:** Uteroferrin (Uf) is the purple acid phosphatase from porcine uterus and contains a coupled dinuclear iron unit. The reduced form [Fe(III),Fe(II)] is pink ($\lambda_{max}$ = 510 nm), is catalytically active toward phosphate ester hydrolysis, and has EPR signals ($g_{av}$ = 1.74) characteristic of an $S = {}^1/_2$ ground state arising from a mixed-valence metal site. The Fe(II) site can be replaced with Zn(II) resulting in an Fe(III),Zn(II) form which is catalytically active, retains a purple color ($\lambda_{max}$ = 530 nm), and has EPR signals characteristic of high-spin Fe(III). Anions such as phosphate, arsenate, and molybdate bind to FeZnUf and $Uf_r$ with similar affinities, resulting in the inhibition of phosphate ester hydrolysis. The spectroscopic changes elicited upon binding of these anions to either $Uf_r$ or FeZnUf afford new insights into the coordination chemistry of the dinuclear site. EPR experiments with $^{17}O$-labeled phosphate provide the first evidence for direct coordination of phosphate to this novel dinuclear metal active site, while the effects on $H_2O/D_2O$ substitution of the EPR spectrum of $Uf_r \cdot AsO_4$ support a model wherein binding of phosphate and arsenate entails at least some proton transfer from the anion to the hydroxo bridge. These results, when extrapolated to the enzyme–substrate interaction, suggest a novel role for the dinuclear unit in the hydrolysis of phosphate esters.

Purple acid phosphatases (PAPs) have been isolated from a wide variety of animal and plant sources,[1] with the best characterized enzymes isolated from porcine uterus (also called uteroferrin, "Uf")[2,3] and bovine spleen.[4,5] These two mammalian enzymes contain an antiferromagnetically coupled dinuclear iron site which can be obtained in two oxidation states.[6] The oxidized form ($Uf_o$) is purple ($\lambda_{max}$ = 550 nm; $\epsilon$ = 4000 $M^{-1}$ $cm^{-1}$), catalytically inactive toward phosphate ester hydrolysis, and EPR silent. Magnetic susceptibility measurements of the oxidized form have indicated strong antiferromagnetic coupling ($\mathcal{H} = -2JS_1 \cdot S_2$) between two high-spin Fe(III) ions with $-2J$ estimated to be between 80 and 300 $cm^{-1}$.[2,4,5,7,8] The reduced form ($Uf_r$) is pink ($\lambda_{max}$ = 510 nm; $\epsilon$ = 4000 $M^{-1}$ $cm^{-1}$), catalyzes phosphate ester hydrolysis, and exhibits EPR signals with $g$ values at 1.94, 1.76, and 1.56 which are characteristic of an $S = {}^1/_2$ ground state arising from antiferromagnetic coupling between a high-spin ferric ion and a high-spin ferrous ion.[2,4,9] Recent SQUID magnetization studies[10] have determined the antiferromagnetic coupling to be

(1) (a) Antanaitis, B. C.; Aisen, P. *Adv. Inorg. Biochem.* **1983**, *5*, 111–136. (b) Doi, K.; Antanaitis, B. C.; Aisen. P. *Struct. Bonding (Berlin)* **1988**, *70*, 1–26.
(2) Antanaitis, B. C.; Aisen, P.; Lilienthal, H. R. *J. Biol. Chem.* **1983**, *258*, 3166–3172.
(3) Antanaitis, B. C.; Aisen, P.; Lilienthal, H. R.; Roberts, R. M.; Bazer, F. W. *J. Biol. Chem.* **1980**, *255*, 11204–11209.
(4) Averill, B. A.; Davis, J. C.; Burman, S.; Zirino, T.; Sanders-Loehr, J.; Loehr, T. M.; Sage, J. T.; Debrunner, P. G. *J. Am. Chem. Soc.* **1987**, *109*, 3760–3767.
(5) Davis, J. C.; Averill, B. A. *Proc. Natl. Acad. Sci. U.S.A.* **1982**, *79*, 4623–4627.
(6) Campbell, H. D.; Dionysius, D. A.; Keough, D. T.; Wilson, B. E.; deJersey, J.; Zerner, B. *Biochem. Biophys. Res. Commun.* **1978**, *82*, 612–620.
(7) Sinn, E.; O'Connor, C. J.; deJersey, J.; Zerner, B. *Inorg. Chim. Acta* **1983**, *78*, L13–L15.
(8) Lauffer, R. B.; Antanaitis, B. C.; Aisen, P.; Que, L., Jr. *J. Biol. Chem.* **1983**, *258*, 14212–14218.
(9) Debrunner, P. G.; Hendrich, M. P.; deJersey, J.; Keough, D. T.; Sage, J. T.; Zerner, B. *Biochim. Biophys. Acta* **1983**, *745*, 103–106.

0002-7863/90/1512-6455$02.50/0 

weak ($-2J$ = 19.8 $cm^{-1}$) in the reduced form, which is consistent with previous NMR[8] and EPR studies.[2,4] The observed weak antiferromagnetic coupling is comparable to that of semimethemerythrin[11] and suggests that $Uf_r$, like semimet$HrN_3$, has a hydroxo-bridged dinuclear iron site.[12] Resonance Raman studies have demonstrated that the color associated with these proteins is a result of a tyrosinate-to-Fe(III) charge-transfer transition.[4,13] The absence of a large change in the extinction coefficient upon reduction indicates that tyrosine is coordinated only to the iron which remains Fe(III) in both forms of the enzyme.[2] Histidine coordination to both metal sites has been indicated by NMR[8] and pulsed EPR[14] studies.

A related enzyme from plant sources is the phosphatase from red kidney bean[15] which Beck et al.[16] have shown to contain one Fe atom and one Zn atom per molecule of protein. The enzyme has a visible spectrum with a $\lambda_{max}$ = 560 nm ($\epsilon$ = 3360 $M^{-1}$ $cm^{-1}$) indicating a possible phenolate–Fe(III) interaction and an EPR spectrum with signals centered at $g$ = 4.3, characteristic of a rhombic high-spin Fe(III) ion.[17] The FeZn kidney bean enzyme can be converted to a catalytically active Fe(II),Fe(III) form by dialysis with ferrous sulfate. The EPR spectrum of this form is similar to that of $Uf_r$, indicating that these enzymes have similar active sites.[18] Similar FeZn forms of uteroferrin[19] and beef spleen purple acid phosphatase[5] have been prepared. These FeZn derivatives have catalytic properties that are similar to those of the native enzymes such as $V_{max}$ and $K_m$ for $p$-nitrophenyl phosphate and $K_i$ for inhibition by phosphate.

The interaction of phosphate with $Uf_r$ is complex. Anaerobic addition of saturating amounts of phosphate to $Uf_r$ gives an enzymatically active complex that is purple and has dramatically different EPR properties.[10] Magnetic susceptibility studies have shown that the antiferromagnetic coupling between the metal sites is significantly reduced upon binding of phosphate to $Uf_r$;[10] this phenomenon causes the EPR signal of the resulting reduced phosphate complex to be quite broad and difficult to observe. Other tetraoxo anions also elicit changes in the properties of uteroferrin.[20] In this study, we compare the effects of phosphate, arsenate, and molybdate on the properties of $Uf_r$ and its Fe(II-I),Zn(II) derivative to gain insight into the interaction of anionic inhibitors with the dinuclear iron site of uteroferrin and relate them to the mechanism for phosphate ester hydrolysis that is catalyzed by a dinuclear metal site. In the case of phosphate, the evidence demonstrates direct coordination of phosphate to the Fe(III) site of the dinuclear iron cluster.

## Experimental Section

**Purification of Uteroferrin.** Uteroferrin was purified as previously described.[21,22] The acid phosphatase activity was determined in 0.1 M acetate buffer, pH 4.9 at 25 °C, with $p$-nitrophenyl phosphate (10 mM) as substrate. The release of the product was measured at 390 nm ($\Delta\epsilon$ = 343 $cm^{-1}$ $M^{-1}$). Purified $Uf_r$ had specific activities of 350–500 U/mg (1 Unit = 1 $\mu$mol/min·mg) and $A_{280}/A_{\lambda max}$ of 13 to 14. The enzyme can be further activated by treatment with $\beta$-mercaptoethanol and catalytic amounts of Fe(II).[19] The FeZn form of uteroferrin was prepared using the method of Keough et al.[19] Metal analysis was obtained by inductively coupled plasma emission spectroscopy performed at the Soil Science Department facility of the University of Minnesota.

**Anion Complexes.** $K_i$ values for the inhibition of $Uf_r$ and FeZnUf by phosphate, arsenate, and molybdate were determined by standard Michaelis–Menten kinetics methods. EPR samples of phosphate or arsenate complexes of $Uf_r$ and FeZnUf were prepared by addition of concentrated anion solutions to degassed protein solutions (0.3–0.6 mM) to give a final anion concentration of 5–10 times $K_i$. Molybdate samples were prepared by addition of 1.1 molar equiv of $Na_2MoO_4$ to a concentrated enzyme solution. The pH of the anion solutions was adjusted to pH 4.9 prior to addition to the protein solution. Protein solutions were degassed prior to anion addition by repeated freeze–pump–thaw cycles. All samples for EPR were prepared under argon to prevent oxidation (for $Uf_r$·$PO_4$ and $Uf_r$·$AsO_4$) and observation of EPR signals associated with molecular oxygen. EPR samples in $D_2O$ or $H_2O$ were prepared by repeated concentration and subsequent dilution in a centricon (Amicon) under an argon atmosphere. Samples of identical concentration (0.2–0.5 mM) in $H_2O$ or $D_2O$ were then loaded into matched quartz EPR tubes.

**$^{17}O$-Containing Samples.** Prior to use 48.6% enriched [$^{17}O$]water (MSD isotopes) was distilled in a microdistillation apparatus. $^{17}O$-labeled phosphate was prepared by reaction of [$^{17}O$]water with $PCl_5$ under nitrogen. The exothermic reaction gave off HCl which was vented through a saturated bicarbonate solution. The solution was then gently heated to remove more HCl. The resulting phosphoric acid solution was neutralized with $NaHCO_3$ and adjusted to pH 5 with concentrated acetate buffer. [$^{16}O$]Phosphate was made in an analogous manner in order to make the samples as similar as possible. [$^{17}O$]Phosphate or [$^{16}O$]phosphate was added to the same protein solution (0.4 mM) in two matched quartz EPR tubes to give a final concentration of 50 mM phosphate.

**$Na_2[Fe^{III}Zn^{II}(HXTA)(OAc)_2]$.** This complex was prepared by reaction of 1 equiv of ferric nitrate with 1 equiv of the ligand, $N,N'$-(2-hydroxy-5-methyl-1,3-xylylene)bis($N$-(carboxymethyl)glycine)[23] in ethanol to form the monoiron complex and subsequent addition of 1 equiv of Zn-$(OAc)_2$. Although this particular complex has not been structurally characterized by X-ray crystallography, it was synthesized by a procedure similar to that of the FeZn complex of the related dinucleating ligand, 2,6-bis[(bis(2-pyridylmethyl)amino)methyl]-4-methylphenol (BPMP).[24] The spectroscopic properties of the HXTA complex is consistent with a structure analogous to that of the BPMP complex.

**EPR Spectroscopy.** EPR spectra were run in 5-mm (o.d.) quartz tubes on a Varian E-109 X-band EPR spectrometer equipped with an Oxford ESR-10 cryostat, a Hewlett-Packard Model 436A frequency counter, and a Hewlett-Packard Model 5350B power meter. Spin quantitations of EPR signals with $g_{av} < 2$ were performed by double integrations of the first derivative spectrum while the use of copper sulfate as a standard with appropriate corrections for differences in $g$ values between the standard and the sample.[25] Integrations of $Uf_r$·$PO_4$ and $Uf_r$·$AsO_4$ were more easily performed when $Uf_r$ was used as the standard, presumably because the saturation behavior of these signals is more similar to that of $Uf_r$ than to that of copper sulfate. For EPR signals near $g$ = 4.3, $Fe^{III}$EDTA was used as the standard for the EPR quantitation.

The energy gap between the first excited state and the ground state, $\Delta$, was estimated by determining the temperature dependence of the power saturation of the signal according to previously published procedures.[11b,26] The slope of the ln $P_{1/2}$ (power at half-saturation) vs $1/T$ plot is equal to $-\Delta$, which corresponds to $-3J$ for a coupled (5/2,2) system ($\mathcal{H} = -2JS_1 \cdot S_2$). Temperatures for this study were read directly off the Oxford temperature controller.

EPR spectra of high-spin ferric complexes were analyzed using the spin Hamiltonian,

$$\mathcal{H} = \mathcal{H}_{Zeeman} + \mathcal{H}_{zero\ field} \quad (1)$$

where $\mathcal{H}_{zero\ field} = D[S_z^2 - {}^1/_3(S(S+1)) + (E/D)(S_x^2 - S_y^2)]$ and $\mathcal{H}_{Zeeman} = \beta_e S_0 g_0 B$. $D$ and $E/D$ are zero-field splitting parameters and the other parameters have their usual definitions. $E/D$ values usually

(10) Day. E. P.; David, S. S.; Peterson, J.; Dunham, W. R.; Bonvoisin, J. J.; Sands, R. H.; Que, L., Jr. *J. Biol. Chem.* **1988**, *263*, 15561–15567.
(11) (a) Maroney, M. J.; Lauffer, R. B.; Que, L., Jr.; Kurtz, D. M., Jr. *J. Am. Chem. Soc.* **1984**, *106*, 6445–6446. (b) Pearce, L. L.; Kurtz, D. M.; Xia, Y.-M.; Debrunner, P. G. *J. Am. Chem. Soc.* **1987**, *109*, 7286–7293.
(12) Scarrow, R. C.; Maroney, M. J.; Palmer, S. M.; Que, L., Jr.; Roe, A. L.; Salowe, S. P.; Stubbe, J. *J. Am. Chem. Soc.* **1987**, *109*, 7857–7864.
(13) (a) Antanaitis, B. C.; Strekas, T.; Aisen, P. *J. Biol. Chem.* **1982**, *257*, 3766–3770. (b) Gaber, B. P.; Sheridan, J. P.; Bazer, F. W.; Roberts, R. M. *J. Biol. Chem.* **1979**, *254*, 8340–8342.
(14) Antanaitis, B. C.; Peisach, J.; Mims, W. B.; Aisen, P. *J. Biol. Chem.* **1985**, *260*, 4572–4574.
(15) Nochumson, S.; O'Rangers, J. J.; Dimitrov, N. V. *Proc. Soc. Exp. Biol. Med.* **1973**, *144*, 527–529.
(16) Beck, J. L.; McConachie, L. A.; Summors, A. C.; Arnold, W. N.; deJersey, J.; Zerner, B. *Biochim. Biophys. Acta* **1986**, *869*, 61–68.
(17) Beck, J. L.; deJersey, J.; Zerner, B.; Hendrich, M. P.; Debrunner, P. G. *J. Am. Chem. Soc.* **1988**, *110*, 3317–3318.
(18) Beck, J. L.; McArthur, M. J.; deJersey, J.; Zerner, B. *Inorg. Chim. Acta* **1988**, *153*, 39–44.
(19) Keough, D. T.; Dionysius, D. A.; deJersey, J.; Zerner, B. *Biochem. Biophys. Res. Commun.* **1980**, *94*, 600–605.
(20) Aisen, P.; Antanaitis, B. C. *J. Biol. Chem.* **1985**, *260*, 751–756.
(21) Pryz, J. W.; Sage, T. J.; Debrunner, P. G.; Que, L., Jr. *J. Biol. Chem.* **1986**, *261*, 11015–11020.
(22) Basha, S. M. M.; Bazer, F. W.; Geisert, R. D.; Roberts, R. M. *J. Anim. Sci.* **1980**, *50*, 113–123.
(23) Schwarzenbach, G.; Anderegg, G.; Sallmann, R. *Helv. Chim. Acta* **1952**, *35*, 1785–1792.
(24) Borovik, A. S.; Papaefthymiou, V.; Taylor, L. F.; Anderson, O. P.; Que, L., Jr. *J. Am. Chem. Soc.* **1989**, *111*, 6183–6195.
(25) Aasa, R.; Vångaard, T. *J. Magn. Reson.* **1975**, *19*, 308.
(26) (a) Rutter, R.; Hager, L. P.; Dhonau, H.; Hendrich, M. P.; Valentine, M.; Debrunner, P. *Biochemistry* **1984**, *23*, 6809–6816. (b) Yim, M. B.; Kuo, L. C.; Makinen, M. W. *J. Magn. Reson.* **1982**, *46*, 247–256.

**Table I.** Resonance Raman Data

| form | 200–1000 region[a] ($cm^{-1}$) | | | | C–H bend ($cm^{-1}$) | C–O stretch ($cm^{-1}$) | ring stretch ($cm^{-1}$) | | ref |
|---|---|---|---|---|---|---|---|---|---|
| $Uf_r$ | | | 803 | 873 | 1173 | 1293 | 1504 | 1607 | 13b |
| $Uf_r$ | | 571 | 806 | 870 | 1169 | 1293 | 1504 | 1604 | 13a |
| $Uf_o$ | | 575 | 805 | 872 | 1168 | 1285 | 1503 | 1603 | 13a |
| FeZnUf | 520 | 572 | 806 | 870 | 1171 | 1284 | 1505 | 1608 | *b* |
| $Uf_r \cdot MoO_4$ | | 573 | 807 | 869 | 1169 | 1287 | 1505 | 1607 | *c* |
| $BPAP_o$[d] | 521 | 574 | 804 | 869 | 1164 | 1281 | 1497 | 1597 | 4 |
| $BPAP_r$[d] | 518 | 574 | 803 | 869 | 1164 | 1287 | 1498 | 1600 | 4 |

[a] All resonances observed in this region are not included. Only the resonances described in text for FeZnUf are listed from other studies. [b] This work. [c] Unpublished data: Pyrz, J. W.; Que, L., Jr. [d] BPAP refers to the purple acid phosphatase isolated from beef spleen (4), and the subscripts o and r refer to oxidized and reduced BPAP, respectively.

can be determined from the $g$ values if $|D| \gg \beta_e g_0 B_0$. Under these conditions, interactions between doublets can be ignored. In the presence of a ligand containing a nuclear spin, such as $^{17}O$, an additional term must be added to the spin Hamiltonian. This hyperfine term describes the interaction between the electron spin and the nuclear spin of the ligand, i.e.

$$\mathcal{H}_{\text{hyperfine}} = I_L \cdot A_L \cdot S \qquad (2)$$

where $I_L$ = nuclear spin of ligand and $A_L$ = hyperfine coupling constant. For $^{17}O$-labeled phosphate that coordinates directly to the metal site, the hyperfine term results in a broadened EPR spectrum due to the interaction between the electron spin and the $I = {}^5/_2$ nuclear spin of the $^{17}O$. Theoretically, a splitting of the resonance by $^{17}O$ is expected; however, the effect is usually too small for splitting to be resolved, and only broadening is observed.[27]

**UV–Visible Spectroscopy.** UV–vis spectra were obtained on either a Cary 219 spectrophotometer or an HP8450 diode array spectrophotometer. Enzyme concentrations were determined by using the extinction coefficient of the visible $\lambda_{max}$ (Uf, $\epsilon$ = 4000 $M^{-1}$ $cm^{-1}$;[6] FeZnUf, $\epsilon$ = 2000 $M^{-1}$ $cm^{-1}$). The extinction coefficient for FeZnUf was determined on samples having a 1:1 Fe–Zn content by normalizing absorbance measurements at 530 nm with the metal content as measured by inductively coupled plasma emission.

**Resonance Raman Spectroscopy.** Resonance Raman spectra were obtained using Spectra-Physics Models 171 argon ion and 375B dye lasers. The spectra were recorded in 2-$cm^{-1}$ steps using a Spex Industries Model 1403 spectrometer interfaced with a Spex Datamate. Spectra were collected at 90° with a constant slit width of 4 $cm^{-1}$. Protein solutions of approximately 0.5 mM were placed in a quartz spinning cell and were cooled to 4 °C by blowing cold nitrogen gas on the spinning cell. Raman samples contained 0.1 M potassium sulfate as an internal standard, and the Raman features recorded were referenced to sulfate $A_1$ stretch at 983 $cm^{-1}$.

## Results

**Comparison of the Fe(III),Fe(II) and Fe(III),Zn(II) Forms of Uteroferrin.** Zerner and his co-workers reported that brief exposure of $Uf_r$ to dithionite and subsequent chromatography on Sephadex G25 yields a "one-iron" form of uteroferrin which has limited stability and no acid phosphatase activity. Subsequent addition of $Zn^{2+}$ and $\beta$-mercaptoethanol regenerates virtually all the enzyme activity within 24 h, and the new active species has been described as an FeZn form of Uf.[19]

Following Zerner's procedure, $Fe^{III}Zn^{II}Uf$ was prepared which exhibited 80–90% of the original enzyme activity. Metal analysis reproducibly gave values of 1.0 ± 0.1 Fe and 1.0 ± 0.1 Zn atoms per molecule of the FeZn protein. Though some samples contained slightly more Fe or Zn, treatment with 10 mM EDTA afforded samples with an Fe/Zn ratio of 1 with only a 5% loss in enzyme activity. FeZnUf exhibits a visible spectrum with $\lambda_{max}$ at 530 nm ($\epsilon$ = 2000 $M^{-1}$ $cm^{-1}$), similar to but distinct from those of $Uf_r$ and $Uf_o$. The observed color presumably arises from a tyrosinate-to-Fe(III) charge-transfer transition, but the difference between the extinction coefficients for the native and FeZn enzymes indicates the ferric sites are not completely identical in these two forms of the protein. Similar visible spectral properties have been reported for the FeZn form of beef spleen purple acid phosphatase ($\lambda_{max}$, 550 nm; $\epsilon$, 2100 $M^{-1}$ $cm^{-1}$).[5] In contrast, Zerner et al. have reported a markedly higher $\epsilon_m$ of 3648 $M^{-1}$ $cm^{-1}$ for their preparations of FeZnUf.[28]

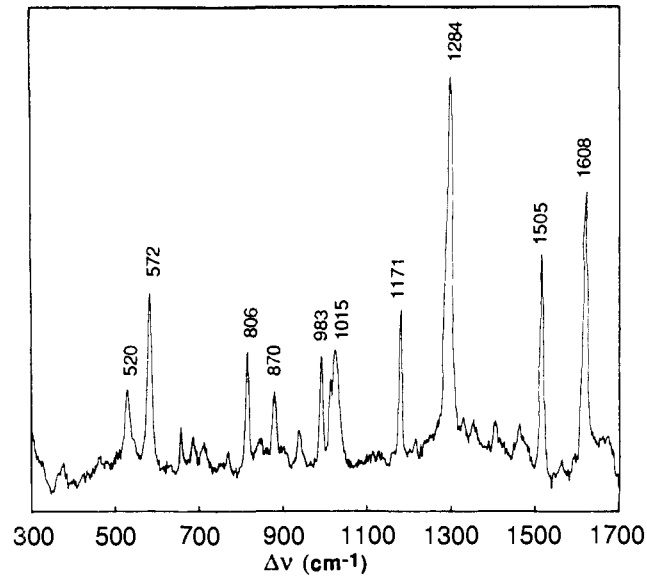


**Figure 1.** Resonance Raman spectrum of FeZnUf. Experimental conditions: 514.5-nm excitation, 200-mW power, 4-$cm^{-1}$ slit width, 0.5-mM enzyme concentration.

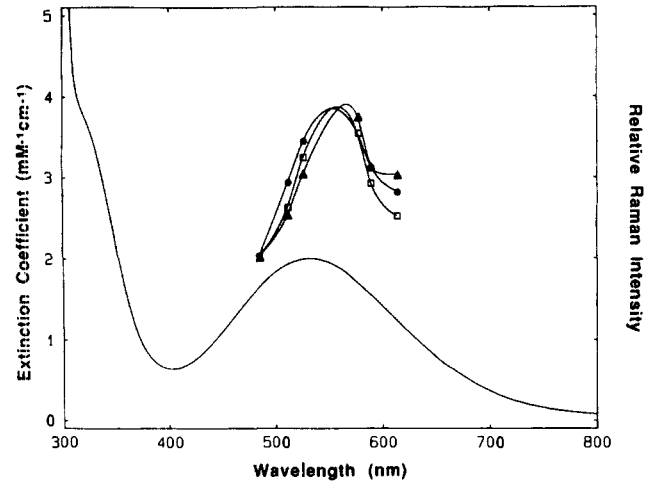


**Figure 2.** Excitation profile for 1284-$cm^{-1}$ (▲), 1505-$cm^{-1}$ (□), and 1608-$cm^{-1}$ (●) peaks superimposed on the visible absorption spectrum (solid line) of FeZnUf. Enhancement was calculated from the height of the sample peak relative to the height of the 983-$cm^{-1}$ sulfate peak and normalized to the same value at 488-nm excitation.

The participation of tyrosinate as a ligand to the metal site in metalloproteins can be identified by the presence of four resonance enhanced tyrosyl vibrations between 1150 and 1650 $cm^{-1}$ upon

(27) Whittaker, J. W.; Lipscomb, J. D. *J. Biol. Chem.* **1984**, *259*, 4487–4495.

(28) Beck, J. L.; Keough, D. T.; DeJersey, J.; Zerner, B. *Biochim. Biophys. Acta* **1984**, *791*, 357–363.

excitation into the visible absorption band.[29] Resonance Raman spectra of FeZnUf (Figure 1) show enhanced tyrosyl vibrations which confirms that the absorption band arises from phenolate-to-Fe(III) charge transfer. Table I compares the resonance Raman data for FeZnUf obtained from this study and those previously reported for uteroferrin and the beef spleen PAP. In accordance with previous studies,[37] the high-frequency bands may be assigned to the following vibrational modes: C–H bending (1171 $cm^{-1}$), C–O stretching (1284 $cm^{-1}$), and ring stretching modes (1505 and 1608 $cm^{-1}$). The excitation profiles of the 1608-, 1505-, and 1284-$cm^{-1}$ bands, as shown in Figure 2, follow that of the absorption band, confirming that the absorption band arises from tyrosinate-to-Fe(III) charge transfer. The high-frequency portion is remarkably similar to that previously reported for oxidized and reduced uteroferrin.[13] In native uteroferrin, the major difference between the oxidized and reduced enzymes is observed in the energy of the C–O stretching vibration which is shifted 8 $cm^{-1}$ higher in energy in the reduced protein. The energy of the C–O stretch in FeZnUf is more similar to that of the oxidized diiron enzyme. When compared to previously reported spectra of oxidized and reduced uteroferrin,[13a] the C–O stretch in FeZnUf, $Uf_r$ (not shown), and $Uf_o$ (not shown) appear as sharp features. Similarly sharp features are observed for the bovine enzyme.[4] These observations are consistent with recent NMR evidence[30] that has suggested that there is only one tyrosinate ligand to the metal site in uteroferrin. Possibly the broadness previously observed was due to a heterogeneous sample which contained a mixture of $Uf_o$ and $Uf_r$.

Low-frequency modes were also observed for FeZnUf at 870, 806, 572, and 520 $cm^{-1}$ (Figure 1) which had previously been observed in native uteroferrin[13] and the purple acid phosphatase from beef spleen.[4] The 806- and 872-$cm^{-1}$ bands were assigned to a metal-coordinated tyrosyl Fermi doublet, and the 575-$cm^{-1}$ feature was assigned to a combination mode with a significant Fe–O stretching contribution.[4,13a,31] The feature at 520 $cm^{-1}$ may be associated with an Fe–OH vibrational mode, by analogy to a similar feature found in the bovine and porcine diiron PAPs.[4,32]

Figure 3 shows the EPR spectrum of $Fe^{III}Zn^{II}Uf$ consisting of a dominant signal near $g = 4.3$; this signal is readily observed up to 220 K, indicative of a slow electron relaxation rate expected of a high-spin Fe(III) center.[33,34] These EPR properties are distinct from those associated with reduced uteroferrin (signals with $g_{av} < 2$ and unobservable above 40 K), confirming that the catalytic activity observed is due to FeZnUf and not to contaminating $Uf_r$. The observed signals for FeZnUf are similar to those of a model compound $Na_2[Fe^{III}Zn^{II}(HXTA)(OAc)_2]$, both of which have somewhat unusual shapes. The observed $g$ values have been analyzed using the spin Hamiltonian for an $S = {}^5/_2$ system and are consistent with a high-spin ferric ion in a nearly rhombic environment. The EPR spectra of most high-spin ferric compounds can be analyzed by neglecting energy shifts caused by field-dependent mixing between different doublets when $|D| \gg g\beta B_0$. However, in these cases, the observed EPR spectrum does not fit the simplified theory exactly because the $|D|$ value appears comparable to $g\beta B_0$. The value of $D$ for the model compound $Na_2[FeZn(HXTA)(OAc)_2]$ has been shown to be small by Mössbauer spectroscopy ($0.2 \pm 0.1$ $cm^{-1}$),[35] and, since the EPR signals are similar, it is likely that the $D$ value for FeZnUf is also small. Simulation of the spectra of FeZnUf and the model FeZn compound will be required to obtain precise $g$ values and values for $E/D$ and $D$. In addition to the signals at $g = 4.3$ arising from a rhombic Fe(III) center, FeZnUf exhibits signals at $g \sim 8.7$ and 7.8 which correspond to other $E/D$ values; their relative intensities suggest that they are minority components. The source of this heterogeneity is not presently understood; indeed the EPR spectra of the bovine and porcine PAPs and the FeZnPAP from red kidney bean also indicate the presence of two species.[4,17] A complete understanding of the EPR properties of FeZnUf will require further investigation, possibly including parallel Mössbauer and magnetic susceptibility studies.

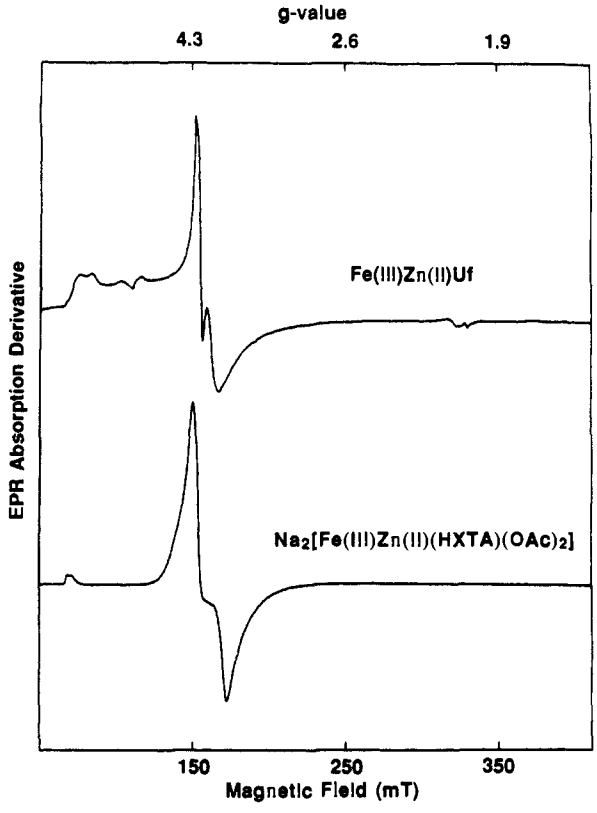


Figure 3. EPR spectra of FeZnUf and $Na_2[FeZn(HXTA)(OAc)_2]$. The spectra have been normalized to give the same signal height. Conditions: 9.2-GHz microwave frequency, 0.2-mW microwave power, 10-G modulation amplitude, 2.5 K. FeZnUf: 0.6 mM, $8 \times 10^2$ receiver gain. $Na_2[FeZn(HXTA)(OAc)_2]$: ~1 mM, $2 \times 10^2$ receiver gain.

**Effect of Anion Binding. Phosphate.** Phosphate[36] is a weak competitive inhibitor for $Uf_r$ ($K_i \sim 14$ mM,[37] $K_d \sim 6$ mM[38]), which requires reversible binding of phosphate to $Uf_r$. In contrast, $Uf_o{\cdot}PO_4$ has a tightly bound phosphate which cannot be removed by gel filtration or dialysis.[38] In order to corroborate the reversibility of phosphate binding to $Uf_r$, the enzyme activity and the $Uf_r$ EPR signal intensity of several samples were monitored during the processes of addition and subsequent removal of phosphate. Anaerobic addition of 10 mM $PO_4$ at pH 5 causes a loss of 75% of the native $Uf_r$ EPR signal. After removal of phosphate by anaerobic passage through Sephadex G25, the native EPR signal is completely recovered. The enzyme activity remains relatively constant throughout this experiment. About 10% of the enzyme activity is lost immediately upon addition of phosphate due to the denaturation of protein upon phosphate addition. Since the native EPR signal is regenerated and the enzyme activity is still intact after passage through Sephadex G25, it is clear that $Uf_r$ is regenerated. This experiment clearly shows that the interaction of

(29) Que, L., Jr. *Coord. Chem. Rev.* **1983**, *50*, 73–108.
(30) Scarrow, R. C.; Pyrz, J. W.; Que, L., Jr. *J. Am. Chem. Soc.* **1990**, *112*, 657–665.
(31) Pyrz, J. W.; Roe, A. L.; Stern, L. J.; Que, L., Jr. *J. Am. Chem. Soc.* **1985**, *107*, 614–620.
(32) Backes, G.; Sanders-Loehr, J.; Loehr, T.; Aisen, P.; David, S. S.; Que, L., Jr. Manuscript in preparation.
(33) Abragam, A.; Bleaney, B. *Electron Paramagnetic Resonance in Transition Metal Ions*; Dover Publications: New York, 1970; pp 133–217.
(34) EPR studies of the bovine FeZnPAP have also been reported;[5] it was noted that the signal at $g = 4.3$ was easily saturated (above 0.25 mW at 13 K) and broadened rapidly above 30 K. The broadening above 30 K is inconsistent with our data and the expected behavior of a high-spin Fe(III) center.
(35) Unpublished results communicated by C. Juarez-Garcia and E. Münck.
(36) The abbreviations that we have adopted for phosphate, arsenate, and molybdate are $PO_4$, $AsO_4$, and $MoO_4$. These abbreviations are not meant to suggest anything about the protonation state of the bound anions.
(37) Pyrz, J. W. Ph.D. Dissertation, Cornell University, 1986.
(38) Keough, D. T.; Beck, J. L.; deJersey, J.; Zerner, B. *Biochem. Biophys. Res. Commun.* **1982**, *108*, 1643–1648.

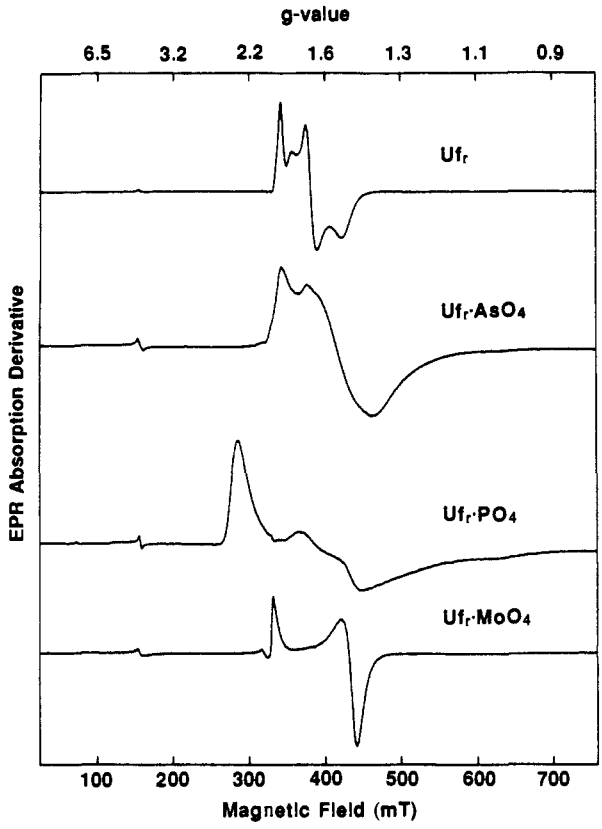


**Figure 4.** EPR spectra of Uf$_r$ and its arsenate, phosphate, and molybdate complexes. The spectra have been normalized to give the same signal height. Experimental conditions: 9.2-GHz microwave frequency. Uf$_r$ and Uf$_r$·MoO$_4$: 0.20-mW microwave power, 10-G modulation amplitude, 8 K, 0.4-mM enzyme concentration, 2 × $10^3$ receiver gain. Uf$_r$·AsO$_4$: 0.20-mW microwave power, 25-G modulation amplitude, 3 K, 0.4-mM concentration, 3.2 × $10^3$ receiver gain. Uf$_r$·PO$_4$: 80-mW microwave power, 25-G modulation amplitude, 2.3 K, 0.6 mM concentration, 2.5 × $10^2$ receiver gain.

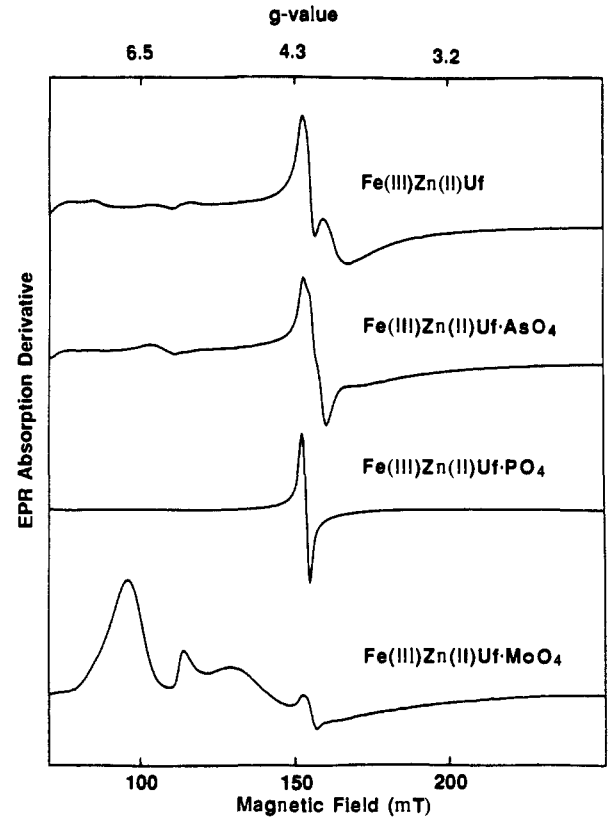


**Figure 5.** EPR spectra of FeZnUf and its arsenate, phosphate, and molybdate complexes. The spectra have been normalized to give the same signal height. Conditions: 9.2-GHz microwave frequency, 10-G modulation amplitude, 3 K. FeZnUf: 0.6-mM concentration, 8 × $10^2$ receiver gain, 0.2-mW microwave power. FeUf·AsO$_4$: 0.2 mM concentration, 2.5 × $10^3$ receiver gain, 0.2-mW microwave power. FeZnUf·PO$_4$: 0.4-mM concentration, 2.5 × $10^2$ receiver gain, 0.065-mW microwave power. FeZnUf·MoO$_4$: 0.5-mM concentration, 3.2 × $10^3$ receiver gain, 0.065-mW microwave power.

phosphate with Uf$_r$ is reversible and that understanding the properties of Uf$_r$·PO$_4$ is important for elucidating the enzyme mechanism for phosphate ester hydrolysis.

The EPR signal of Uf$_r$·PO$_4$ has recently been reported.[10] Under conditions of low power which are optimum for Uf$_r$ (microwave power, 0.2 mW; temperature, 8 K; modulation amplitude, 10 G), the EPR spectrum of the phosphate complex is not readily observed. In contrast, the EPR signal of Uf$_r$·PO$_4$ is readily observed under conditions (microwave power, 1 mW; temperature, 2 K; modulation amplitude, 25 G) wherein the Uf$_r$ signal is severely saturated. The drastic changes in EPR properties observed upon phosphate binding to Uf$_r$ (Figure 4) are a conseqence of the significant decrease in $J$. The Uf$_r$·PO$_4$ EPR signal is difficult to saturate even at 2 K in contrast to that of Uf$_r$ which saturates at microwatt power at 2 K; this behavior is consistent with an Orbach relaxation process in which the accessibility of the excited state facilitates electron relaxation. As the temperature is increased from 2 to 10 K, the Uf$_r$·PO$_4$ EPR signal intensity diminishes much more rapidly than the Uf$_r$ EPR signal intensity, which is also consistent with a smaller $J$ for Uf$_r$·PO$_4$, so that at higher temperature the ground state is significantly depopulated. The comparison of the EPR signals of the native enzyme and its phosphate complex shows significant perturbation of the metal site upon phosphate binding. Previous difficulties in observation of the Uf$_r$·PO$_4$ EPR signal[20] most likely stem from the fact that its EPR properties are strikingly different from Uf$_r$.

Phosphate is also a weak competitive inhibitor for FeZnUf with a $K_i$ of 3.5 mM. Addition of saturating amounts of phosphate to FeZnUf affects its visible spectrum. The resulting complex has a $\lambda_{max}$ of 550 at pH 6 which red shifts to 562 nm as the pH is lowered to pH 3. This is similar to but not quite as dramatic as what is seen for Uf$_r$·PO$_4$ which has a $\lambda_{max}$ at pH 6 of 530 and a $\lambda_{max}$ at pH 3 of 560 nm. Figure 5 shows that the EPR spectrum of FeZnUf upon phosphate addition has a sharp signal $g$ = 4.3. A significantly weaker signal at $g$ = 9.6 can also be observed at higher gain. These signals are consistent with a high-spin ferric ion in a rhombic environment with the 4.3 and 9.6 signals arising from the middle and ground doublets, respectively. Double integration of the EPR signal at $g$ = 4.3 of FeZnUf·PO$_4$ correlated with the amount of active site bound iron determined from the visible spectrum. Passage of FeZnUf·PO$_4$ through Sephadex G25 to remove phosphate regenerates the characteristic FeZnUf EPR signal, indicating that the interaction of phosphate with FeZnUf is reversible as was observed with Uf$_r$. The fact that phosphate addition affects the EPR and the visible spectra of FeZnUf indicates that the ferric ion is perturbed when phosphate binds to the active site.

**Arsenate.** Arsenate has been shown to interact with Uf$_r$ in a manner similar to that of phosphate.[21] Arsenate, not surprisingly, is also a competitive inhibitor for reduced uteroferrin with a $K_i$ of 1.3 mM[37] and potentiates the aerobic oxidation of Uf$_r$. Aisen and co-workers have reported that addition of saturating amounts of arsenate to Uf$_r$ causes little change in the shape of the native EPR signal but does decrease the intensity by 50%. In our studies, addition of saturating amounts of arsenate to Uf$_r$ broadens the EPR signal (Figure 4) and blue-shifts the phenolate-to-Fe(III) charge-transfer band to 505 nm. Double integration of Uf$_r$·AsO$_4$ at 2.5 K gave 0.97 spin/molecule of protein. Interestingly, this signal is not as broad nor as anisotropic as the EPR signal for the phosphate complex of Uf$_r$, but more so than that of Uf$_r$. The saturation behavior of the EPR signal of Uf$_r$·AsO$_4$ is also intermediate between that of Uf$_r$ and its phosphate complex indicating that the $J$ value is between those of these two forms. The temperature dependence of the EPR saturation allowed the estimation

of $-2J$ for $Uf_r \cdot AsO_4$ to be $12 \pm 1$ cm$^{-1}$ which is, in fact, intermediate between the $-2J$ values determined by magnetization studies for $Uf_r$ (19.8 cm$^{-1}$)[10] and $Uf_r \cdot PO_4$ (6.0 cm$^{-1}$).[10] The three $J$ values are not directly comparable, since the arsenate value was measured using a technique different from the other two; therefore, magnetic susceptibility studies on $Uf_r \cdot AsO_4$ are in progress and should yield a more precise value for $J$.

Arsenate is also a competitive inhibitor for FeZnUf with a $K_i$ of 2.5 mM. Addition of saturating amounts of arsenate to FeZnUf causes a blue shift in the charge-transfer band from 530 to 510 nm. The EPR signal of FeZnUf·$AsO_4$ (Figure 5) is slightly sharper than that of FeZnUf but not as sharp as FeZnUf·$PO_4$. It is interesting that the same trends as observed with arsenate and phosphate with $Uf_r$ are seen with FeZnUf. Phosphate causes a red shift in the phenolate-to-Fe(III) charge-transfer band of both $Uf_r$ and FeZnUf, while arsenate causes a blue shift in the charge-transfer band of the two forms. The EPR signals of the arsenate complex of FeZnUf and $Uf_r$ have properties which are intermediate between those of the respective uncomplexed enzyme and the phosphate complex.

**Molybdate.** Molybdate is a potent competitive inhibitor for $Uf_r$ with a $K_i$ of $4 \pm 2$ $\mu$M (for data see supplementary material). Addition of 1.1 equiv of molybdate to $Uf_r$ causes a slight red shift in the charge-transfer band which is unchanged with time, indicating that molybdate forms an air-stable complex with $Uf_r$.[20] Subsequent addition of phosphate to $Uf_r \cdot MoO_4$ causes no immediate change in the visible spectrum, possibly indicating that molybdate is able to prevent phosphate from binding. However, a very slow conversion to $Uf_o \cdot PO_4$ occurs on the order of days, showing that the metal site is still accessible to phosphate in the presence of molybdate. Molybdate binding changes the rhombic EPR spectrum of $Uf_r$ to an axial species (Figure 4).

The interaction of molybdate with FeZnUf is somewhat unusual. Molybdate is also a potent competitive inhibitor of FeZnUf with a micromolar $K_i$ ($\sim 2$ $\mu$M). Addition of 1.1 equiv of molybdate to FeZnUf causes a blue shift in the charge-transfer band to give a pink complex with a $\lambda_{max}$ = 510 nm, reminiscent of $Uf_r$. Subsequent addition of phosphate to FeZnUf·$MoO_4$ does not perturb the visible spectrum which again suggests that the molybdate is blocking the phosphate binding site as would be expected considering that molybdate binds 1000-fold tighter than phosphate to the metal site. The addition of molybdate to FeZnUf converts the rhombic high-spin ferric site to an axial species with $g$ values at 6.92, 5.85, and 5.06 as shown in Figure 5. These $g$ values can be fit with the spin Hamiltonian to an $E/D = 0.04$ where signals with $g = 6.9$ and 5.1 come from the ground doublet, and the $g = 5.9$ signal arises from the middle doublet. In agreement with the assignment to an excited state, the $g = 5.9$ signal diminishes relative to the $g = 6.9$ and 5.1 signals as the temperature is lowered. In addition, there is a small amount of adventitious iron at $g = 4.3$ which is usually present in uteroferrin samples.

**Evidence for Anion Coordination to the ($\mu$-Hydroxo)diiron Unit. $^{17}O$ Experiments.** ENDOR and ESEEM studies of $Uf_r$·$^{95}MoO_4$ have indicated that molybdate is most likely bound to the diiron site.[39] Phosphate and arsenate have been shown to perturb the spectroscopic properties of the metal site, but direct coordination to the metal site has not been established. A method for establishing phosphate binding to the metal centers in Uf is the use of $^{17}O$-labeled phosphate in EPR experiments.[27] The sharpness of the FeZnUf·$PO_4$ EPR signal at $g = 4.3$ (peak-to-peak width = 2.5 mT) allows such an experiment to be performed. Addition of $^{17}O$-labeled phosphate to FeZnUf results in resonances which are broader by 0.4 mT than the corresponding signals from the [$^{16}O$]phosphate complex as shown in Figure 6. Broadening is apparent in both the $g = 4.3$ and $g = 9.6$ EPR resonances. This type of hyperfine interaction is only observed when there is a direct $^{17}O$ ($I = {}^5/_2$) iron bond.[27] The observation of hyperfine broadening is thus direct evidence for phosphate as a ligand to the Fe(III)

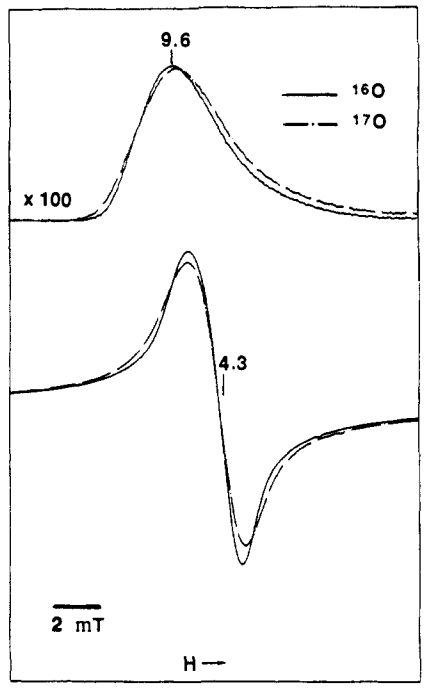


Figure 6. EPR spectra of FeZnUf·$PO_4$ labeled with [$^{16}O$]phosphate and [$^{17}O$]phosphate illustrating the broadening of the resonances in the $^{17}O$-labeled sample. Conditions: 9.2-GHz microwave frequency, 10-G modulation amplitude, 3 K, 0.065-mW microwave power, 0.4-mM concentration; $g = 4.3$, $2.5 \times 10^2$ receiver gain; $g = 9.6$, $2.5 \times 10^4$ receiver gain.

site in FeZnUf. The broadness of the EPR signal of $Uf_r \cdot PO_4$ [$g$ values (line widths in mT) = 1.06 (150), 1.51 (140), 2.27 (110)] precludes doing the analogous experiment with the $^{17}O$-labeled phosphate complex of $Uf_r$. We note also a small shift in $g$ value of the 4.3 and 9.6 signal of the FeZnUf·[$^{17}O$]phosphate complex compared to the FeZnUf·[$^{16}O$]phosphate complex; this particular isotope effect is not currently understood.

**$D_2O$ Effects.** The weakening of the antiferromagnetic coupling in $Uf_r$ upon phosphate binding is proposed to result from a modification of the hydroxo bridge by hydrogen bonding or proton transfer from the anion to the bridge.[10] In fitting the magnetic susceptibility data for $Uf_r \cdot PO_4$ Day et al.[10] found that the $g$ value anisotropy of the coupled Fe(II),Fe(III) center is a very sensitive function of $J$. Indeed, the EPR spectra of the series $Uf_r$, $Uf_r \cdot AsO_4$, and $Uf_r \cdot PO_4$ serve as an excellent illustration of this sensitivity (Figure 4), with the intermediate anisotropy of the $AsO_4$ complex suggestive of a $J$ value intermediate between those of the native enzyme and the phosphate complex. The presence of hydrogen bonding may then be inferred from its effect on $J$ when the EPR spectra in $H_2O$ and $D_2O$ are compared. EPR experiments in $D_2O$ and $H_2O$ containing buffers were performed on $Uf_r$, $Uf_r \cdot AsO_4$, $Uf_r \cdot PO_4$, and $Uf_r \cdot MoO_4$ (Figure 7). The EPR spectrum of $Uf_r \cdot AsO_4$ in $D_2O$–buffer shows noticeably smaller $g$-anisotropy than in $H_2O$. These changes are reproducible and do not result from the difference in pH and pD.[40] In contrast, no changes in the EPR $g$ values are observed for $Uf_r$ and $Uf_r \cdot MoO_4$ in $D_2O$ and $H_2O$. The small changes in the intensity of the $g_x$ features in the $Uf_r$ signal observed may result from a perturbation of the equilibrium between the two forms of $Uf_r$ that exist at pH 4.9.[41] There are also no obvious changes in $Uf_r \cdot PO_4$ in $D_2O$ or $H_2O$ (spectra not shown); owing to the extreme broadness of the EPR signals of $Uf_r \cdot PO_4$, any small changes in $g$ values or signal shape may

(39) Doi, K.; McCracken, J.; Peisach, J.; Aisen, P. *J. Biol. Chem.* **1988**, *263*, 5757–5763.

(40) Similar differences between the $H_2O$ and $D_2O$ samples of $Uf_r \cdot AsO_4$ were observed when pH was equal to pD (pD = pH meter reading + 0.4) and when the pH meter readings of both samples were set to pH 4.9.

(41) The existence of two forms of the bovine purple acid phosphatase has been well-documented and appears to be dependent on pH.[4] Two forms of $Uf_r$ also exist, but the exact relationship between the two forms is not known, though it does appear to be somewhat dependent on pH (David, S. S.; Que, L., Jr. Unpublished results).

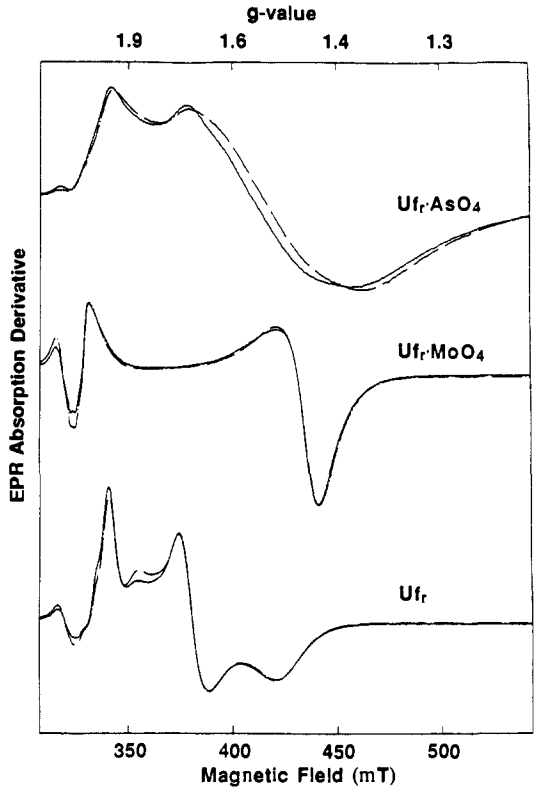


**Figure 7.** EPR spectra of $Uf_r$·$AsO_4$, $Uf_r$·$MoO_4$, and $Uf_r$ in $H_2O$ (—) and $D_2O$ (—). Signals have been normalized to give the same signal height. The heights of one or more features were matched in the overlayed spectra. EPR conditions: 9.2-GHz microwave frequency, 10-G modulation amplitude. $Uf_r$·$AsO_4$: 2.5 K, 0.20-mW microwave power, $8 \times 10^3$ receiver gain, 0.5-mM sample concentration. $Uf_r$: 8 K, 0.20-mW microwave power, $2 \times 10^3$ receiver gain, 0.4-mM sample concentration. $Uf_r$·$MoO_4$: 8 K, 0.20-mW microwave power, $4 \times 10^3$ receiver gain, 0.3-mM sample concentration.

not be observable. These experiments demonstrate that the nature of the solvent isotope affects the *g*-anisotropy (and in turn, the *J* value) of $Uf_r$·$AsO_4$, strongly implicating a hydrogen-bonding interaction to the hydroxo bridge, presumably from the anion. The absence of this effect in $Uf_r$·$MoO_4$ further suggests that molybdate interacts with the dinuclear iron site in a manner significantly different from that of arsenate and phosphate.

## Discussion

The binding of tetraoxo anions to uteroferrin elicits changes in the spectroscopic properties of the dinuclear metal cluster in the active site. The effects provide insight into how such anions, and by extension the substrate, may interact with the metal centers of the enzyme and thus aid in the formulation of a mechanism for phosphate ester hydrolysis by this novel active site. We have investigated anion binding to both the native Fe(III),Fe(II) enzyme as well as its catalytically competent Fe(III),Zn(II) derivative. FeZnUf exhibits nearly 100% of the catalytic activity of the native enzyme and binds the inhibitors phosphate, arsenate, and molybdate with affinities comparable to those of the native enzyme. These properties indicate that the substitution of Zn(II) for Fe(II) does not appreciably affect the catalytic properties of the active site, though it has significantly changed its spectroscopic properties. These different properties allow a comparison of the two sites to be made and provide additional strategies for investigating the coordination chemistry of the individual metal centers.

Metal analysis indicated that there are one Fe and one Zn per molecule of FeZnUf. The curious observation that the extinction coefficient of the phenolate-to-Fe(III) charge-transfer band is half that of the native enzyme might indicate that only half of the molecules have Fe(III) in the phenolate site while the other half have Zn(II). The smaller extinction coefficient is similar to that reported by Averill et al. for the bovine FeZn enzyme[5] but nearly half that reported by Zerner et al. ($\epsilon$ = 3648 $M^{-1}$ $cm^{-1}$) for their

**Table II.** Effects of Anion Binding[a]

| form | $\lambda_{max}$ ($\epsilon$) | major EPR, *g*-values | $-2J$ value[b] |
|---|---|---|---|
| $Uf_r$ | 510 (4000) | 1.56, 1.74, 1.96[c] | 19.8 (5) ($\chi$),[c] 20 (NMR)[d] |
| $Uf_r$·$AsO_4$ ($H_2O$) | 505 (4000) | 1.41, 1.56, 1.92[e] | 12 (EPR) |
| $Uf_r$·$AsO_4$ ($D_2O$) | 505 (4000) | 1.44, 1.62, 1.93[e] | |
| $Uf_r$·$PO_4$ | 536 (4000) | 1.06, 1.51, 2.27[c] | 6.0 (5) ($\chi$)[c] |
| $Uf_r$·$MoO_4$ | 525 (4000) | 1.52, 1.97[c] | 20 (NMR),[f] 15 (EPR) |
| FeZnUf | 530 (2000) | 3.96, 4.27, 4.35[e] 8.7, 7.8[e] | |
| FeZnUf·$AsO_4$ | 510 (2000) | 3.81, 4.17, 4.31[e] 8.8, 6.0[e] | |
| FeZnUf·$PO_4$ | 550 (2000) | 4.25, 4.28, 4.32[e] 9.6[e] | |
| FeZnUf·$MoO_4$ | 510 (2000) | 5.06, 6.92[e] 5.85[e] | |

[a] Unless otherwise indicated, the data from this table are derived from this work. [b] Information in parentheses refers to method for determining $J - \chi$, magnetic susceptibility; NMR, temperature dependence of the isotropic shifts in the NMR; EPR, power saturation behavior as a function of temperature. [c] Reference 10. [d] Reference 8. [e] These *g* values were estimated from the EPR spectrum and do not reflect a fitting of the EPR spectrum. [f] Reference 30.

preparation of FeZnUf.[28] A possible explanation for a lower extinction coefficient could be the presence of a mixture of dinuclear sites. There are a number of observations which argue against scrambling between the two sites. First, the enzymatic activity of FeZnUf is nearly identical with that of the native enzyme. It seems unlikely that combinations of Fe and Zn in either site would have activity identical with that of the native enzyme. Furthermore, active enzyme is not obtained after Zn(II) reconstitution of the apoenzyme.[19] Secondly, the EPR spectrum of FeZnUf·$PO_4$ shows no signals characteristic of $Uf_r$ and integrates to one $S = {}^5/_2$ center per protein molecule. In addition, the activity of FeZnUf is unaffected by addition of hydrogen peroxide in contrast to the native Fe(III),Fe(II) enzyme. These observations coupled with the known strong affinity of phenolate ligands for Fe(III)[29] suggest that Zn(II) occupies the Fe(II) site of the enzyme in FeZnUf. It is clear though that replacement of Fe(II) with Zn(II) somehow perturbs the spectroscopic properties of the site as evidenced by the change in the extinction coefficient of the phenolate-to-Fe(III) charge-transfer band. The reasons for the different extinction coefficients in our preparation and Zerner's are not clear. Interestingly, the extinction coefficient found in our preparation of FeZnUf is that expected for the presence of one iron(III)–phenolate bond based on model studies of Fe(III)–phenolate complexes (1000–2000 $M^{-1}$ $cm^{-1}$);[42] indeed $Uf_r$ and $Uf_o$ have abnormally high extinction coefficients for having only one Fe(III)–tyrosine bond,[30] and the reasons for this are under investigation.

Tetraoxo anions affect the catalytic and spectroscopic properties of uteroferrin, and a comparison of these effects affords important insights into the coordination chemistry of the dinuclear active site. It is interesting that phosphate, arsenate, and molybdate each engender a unique set of effects, but these anions each affect the Fe(III),Fe(II) and Fe(III),Zn(II) enzymes similarly (Table II), suggesting that the anions interact with the active site in a manner that is independent of the nature of the divalent ion. These interactions can be classified from two different perspectives. From a biochemical standpoint, phosphate and arsenate are similar; both are weak competitive inhibitors and potentiate the aerobic inactivation of the diiron enzyme.[21] Molybdate is distinct from the other two in being a strong competitive inhibitor and in forming an air-stable complex with $Uf_r$. From a spectroscopic perspective, phosphate differs from the other two in inducing significantly weaker coupling between the iron centers. Any model that is

(42) (a) Ackerman, G. A.; Hesse, D. Z. *Anorg. Allg. Chem.* **1970**, *375*, 77–86. (b) Gaber, B. P.; Miskowski, V.; Spiro, T. G. *J. Am. Chem. Soc.* **1974**, *96*, 6868–6873. (c) Ainscough, E. W.; Brodie, A. M.; Plowman, J. E.; Brown, K. L.; Addison, A. W.; Gainsford, A. R. *Inorg. Chem.* **1980**, *19*, 3655–3663.

**Scheme I**

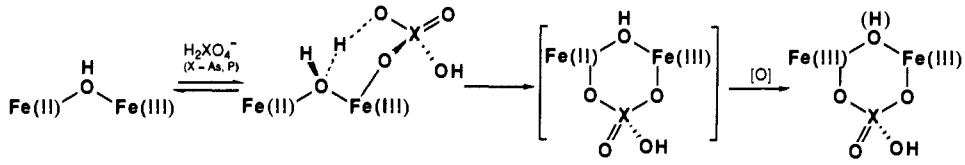


proposed will have to rationalize these differences in behavior.

Anion coordination to the dinuclear site is now firmly established on the basis of the ENDOR and ESEEM studies of Aisen et al.[14] on $Uf_r{\cdot}^{95}MoO_4$ and our observation of $^{17}O$-broadening in the EPR spectrum of $FeZnUf{\cdot}P^{17}O_4$. We would argue that phosphate and molybdate must coordinate to the dinuclear site differently because they affect the enzyme differently both biochemically and spectroscopically. Since molybdate binds to the enzyme three orders of magnitude more strongly than phosphate, we propose that molybdate coordinates in a bidentate mode, perhaps by bridging the metal centers as precedented by $[Fe_2(Me_3TACN)_2O(MoO_4)_2]$.[43] However, spectroscopic proof for this hypothesis is currently unavailable and will require additional studies (e.g., EXAFS and/or Mössbauer studies of $Uf_r{\cdot}MoO_4$ and $FeZnUf{\cdot}MoO_4$). Following this line of argument, we propose that phosphate binds in a monodentate fashion and only to the Fe(III) center of the dinuclear unit. In corroboration, the Mössbauer parameters of the Fe(III) center alone in $Uf_r$ are significantly affected by the addition of phosphate, while the parameters of both Fe(III) centers in $Uf_o$ are altered in $Uf_o{\cdot}PO_4$,[21] where phosphate is tightly bound and believed to bridge the two metals on the basis of EXAFS data.[44]

The differences in the magnetic properties of $Uf_r{\cdot}PO_4$ and $Uf_r{\cdot}MoO_4$ can be explained by altering the $\mu$-hydroxo bridge which mediates the antiferromagnetic coupling between the metal centers in the dinuclear unit. $H_2PO_4^-$ is the dominant form of the phosphate anion at pH 5 and should become more acidic upon binding to the Fe(III) center of $Uf_r$. This proton can hydrogen bond to the $\mu$-hydroxo bridge, thus weakening the antiferromagnetic interaction as shown in Scheme I. The interactions proposed in the scheme are not unprecedented. Protonation of the $\mu$-OH bridge of deoxyhemerythrin has also been proposed to explain the change in the magnetic properties of the dinuclear site upon azide binding,[45] and hydrogen bonding to the oxo bridge is proposed for the bound hydroperoxide ligand in oxyhemerythrin.[46] In addition, direct analogies to the proposed structure for $Uf_r{\cdot}PO_4$ can be found in two synthetic studies. Turpeinen et al.[47] have prepared ($\mu$-aqua)bis($\mu$-carboxylato)dimetal complexes, e.g., $[M^{II}_2(tmen)_2(O_2CR)_2(\mu\text{-}H_2O)(\mu\text{-}RCO_2)_2]$ (M = Co or Ni, tmen = *N,N,N',N'*-tetramethyl-1,2-diaminoethane), which feature an aqua bridge that is hydrogen bonded to the terminal carboxylate groups. Buckingham et al.[48] recently proposed on the basis of $^{31}P$ NMR evidence that the $HPO_4$ ligand must be hydrogen bonded to the OH ligand in *cis*-$[Co(en)_2(HPO_4)(OH)]$. The binding of molybdate to $Uf_r$, on the other hand, is not expected to be accompanied by similar protonation effects because of the predominance of the completely deprotonated $MoO_4^{2-}$ in solution at pH 5 ($pK_a$ 3.7).

The fact that arsenate behaves biochemically much like phosphate suggests that they interact with the active site in similar fashion, but the binding of arsenate to $Uf_r$ induces less dramatic changes in spectroscopic and magnetic properties than phosphate. The EPR spectrum of $Uf_r{\cdot}AsO_4$ exhibits a *g*-anisotropy intermediate between those of $Uf_r$ and $Uf_r{\cdot}PO_4$, and power saturation studies estimate $-2J$ to be $12 \pm 1$ cm$^{-1}$, a value also intermediate between those of $Uf_r$ and $Uf_r{\cdot}PO_4$. These observations suggest that $H_2AsO_4^-$ coordinates to the Fe(III) center of the dinuclear site but hydrogen bonds to the hydroxo bridge more weakly than $H_2PO_4^-$.[49] Such a model is consistent with the observed decrease in *g*-anisotropy in the EPR spectrum of $Uf_r{\cdot}AsO_4$ in $D_2O$ containing buffer. The replacement of a proton with a deuteron in a hydrogen bond should result in a weaker H bond to the $\mu$-hydroxo bridge, which should increase the coupling between the iron centers and afford an EPR spectrum that has decreased *g*-anisotropy. That this effect is absent in $Uf_r$ and $Uf_r{\cdot}MoO_4$ is a consequence of the stronger coupling in these complexes which engenders a smaller *g*-anisotropy and decreases the sensitivity of these signals to such subtle effects.[10] The lack of a $D_2O$ effect on the EPR spectrum of $Uf_r{\cdot}PO_4$ may indicate that proton transfer from anion to hydroxo bridge may be nearly complete. A similar $H_2O/D_2O$ effect has been observed in the resonance Raman spectrum of oxyhemerythrin and is rationalized by hydrogen bonding of the bound hydroperoxide to the $\mu$-oxo bridge.[46]

Subsequent to phosphate (or arsenate) binding, we propose a slow structural rearrangement to form the bridged phosphate complex, which then rapidly oxidizes to $Uf_o{\cdot}PO_4$ in the presence of air. Such a transformation is consistent with suggestions made by Averill et al.[50] that binding of phosphate to the ferrous site potentiates its air oxidation. The phosphate bridges the two ferric ions in $Uf_o{\cdot}PO_4$ on the basis of EXAFS studies[44] and its tight binding to the protein[38] such that only reduction or denaturation of the protein releases it.[38]

In light of the above observations, the mechanism of phosphate ester ($ROPO_3H^-$) hydrolysis by a dinuclear metal site may incorporate features deduced for phosphate binding (Scheme I). Like $H_2PO_4^-$, the substrate may bind in a monodentate manner to the Fe(III) site and interact with the hydroxo bridge. These interactions with the ferric site and the $\mu$-hydroxo bridge should facilitate phosphate ester hydrolysis by promoting metaphosphate formation and release of phenolate. The participation of a metaphosphate intermediate would be consistent with conclusions drawn by Westheimer,[51] Knowles,[52] and others[53] on the hydrolysis of phosphate esters under acidic conditions. Support for such a mechanism may come from the determination of the stereochemical course of phosphate hydrolysis as well as other classic tests for a metaphosphate intermediate.[52,53] While alkaline phosphatases[54] and prostatic acid phosphatases[55] are believed to hydrolyze phosphate esters via a covalent phosphoenzyme intermediate because of the retention of configuration at phosphorus,

(43) Chaudhuri, P.; Winter, M.; Wieghardt, K.; Gehring, S.; Haase, W.; Nuber, B.; Weiss, J. *Inorg. Chem.* **1988**, *27*, 1564–1569.

(44) (a) Kauzlarich, S. M.; Teo, B. K.; Zirino, T.; Burman, S.; Davis, J. C.; Averill, B. A. *Inorg. Chem.* **1986**, *25*, 2781–2785. (b) Que, L., Jr.; Scarrow, R. C. *ACS Symp. Ser.* **1988**, *372*, 152–178.

(45) Reem, R. C.; Solomon, E. I. *J. Am. Chem. Soc.* **1987**, *109*, 1216–1226.

(46) (a) Shiemke, A. K.; Loehr, T. M.; Sanders-Loehr, J. *J. Am. Chem. Soc.* **1986**, *108*, 2437–2443. (b) Shiemke, A. K.; Loehr, T. M.; Sanders-Loehr, J. *J. Am. Chem. Soc.* **1984**, *106*, 4951–4956.

(47) Turpeinen, U.; Hämäläinen, R.; Reedijk, J. *Polyhedron* **1987**, *6*, 1603–1610.

(48) (a) Buckingham, D. A.; Clark, C. R.; Stewart, I. *Aust. J. Chem.* **1989**, *42*, 709. (b) Brasch, N. E.; Buckingham, D. A.; Simpson, J.; Stewart, I. *Inorg. Chem.* **1990**, *29*, 371–377.

(49) If the interactions of phosphate and arsenate with the active site were entirely analogous, $H_2AsO_4^-$ would be expected to protonate the $\mu$-hydroxo bridge more readily because of its slightly higher acidity ($pK_a$ of 7.0 vs 7.2 for $H_2PO_4^-$). However, the two anions are not structurally identical and thus would not necessarily interact with the dinuclear site in exactly the same way.

(50) Burman, S.; Davis, J. C.; Weber, M. J.; Averill, B. A. *Biochem. Biophys. Res. Commun.* **1986**, *136*, 490–497.

(51) (a) Westheimer, F. H. *Chem. Rev.* **1981**, *81*, 313–326. (b) Butcher, W. W.; Westheimer, F. H. *J. Am. Chem. Soc.* **1955**, *77*, 2420–2424.

(52) (a) Friedman, J. M.; Freeman, S.; Knowles, J. R. *J. Am. Chem. Soc.* **1988**, *110*, 1268–1275. (b) Freeman, S.; Friedman, J. M.; Knowles, J. R. *J. Am. Chem. Soc.* **1987**, *109*, 3166–3168.

(53) (a) Bunton, C. A.; Fendler, E. J.; Fendler, J. H. *J. Am. Chem. Soc.* **1967**, *89*, 1221–1230. (b) Kirby, A. J.; Vagolis, A. G. *J. Am. Chem. Soc.* **1967**, *89*, 415–423.

(54) Jones, S.R.; Kindman, L. A.; Knowles, J. R. *Nature* **1978**, *275*, 564–565.

(55) Buchwald, S. L.; Saini, M. S.; Knowles, J. R.; Van Etten, R. L. *J. Biol. Chem.* **1984**, *259*, 2208–2213.

the purple acid phosphatases may employ this unique metal site to catalyze hydrolysis of phosphate esters in a significantly different manner.

**Acknowledgment.** This work was supported by a grant from the National Science Foundation (DMB-8804931). S.S.D. is grateful for a graduate fellowship from the Amoco Foundation. We are also grateful to Dr. J. D. Lipscomb, A. Orville, and M. Harpel for helpful discussions concerning $^{17}O$ experiments. The efforts of Dr. R. E. Norman in the preparation of the $Na_2[FeZn(HXTA)(OAc)_2]$ complex are also appreciated.

**Registry No.** $PO_4^{3-}$, 14265-44-2; $AsO_4^{3-}$, 15584-04-0; $MoO_4^{2-}$, 14259-85-9.

**Supplementary Material Available:** Lineweaver-Burke plots of uteroferrin inhibition by molybdate (2 pages). Ordering information is given on any current masthead page.

# Liquid-Phase ESR, ENDOR, and TRIPLE Resonance of Porphycene Anion Radicals

**Jenny Schlüpmann,[†] Martina Huber,[‡] Moshe Toporowicz,[§] Martin Plato,[†] Matthias Köcher,[⊥] Emanuel Vogel,[⊥] Haim Levanon,[§] and Klaus Möbius*,[†]**

*Contribution from the Institut für Molekülphysik, Freie Universität Berlin, Arnimallee 14, 1000 Berlin 33, West Germany, Institut für Organische Chemie, Freie Universität Berlin, Takustrasse 3, 1000 Berlin 33, West Germany, Department of Physical Chemistry and The Fritz Haber Research Center for Molecular Dynamics, The Hebrew University of Jerusalem, Jerusalem, 91904 Israel, and Institut für Organische Chemie, Universität Köln, Greinstrasse 4, 5000 Köln, West Germany.* *Received November 17, 1989*

**Abstract:** Porphycenes are novel structural isomers of porphyrins. The radical anions of several porphycenes were studied by ESR, ENDOR, and TRIPLE resonance in liquid solution yielding the isotropic hyperfine coupling constants including signs. For the unsubstituted free-base porphycene, the 2,7,12,17-tetra-*n*-propylporphycene, and the 9,10,19,20-tetra-*n*-propylporphycene, the experimental findings are compared with results of all-valence-electrons self-consistent field molecular orbital calculations (RHF-INDO/SP).

## Introduction

The porphyrins and metalloporphyrins constitute the essential chromophores in many photochemical and photobiological processes. It is for this and other reasons that the porphycenes (Figure 1), a new class of planar tetrapyrrolic macrocycles, structurally isomeric to the porphyrins, have invited a thorough study of their physical and chemical properties.[1,2]

Investigations on the role porphycenes may play in photophysical and photochemical processes have just started.[3-5] The difference in molecular structure and symmetry between porphyrins and porphycenes manifests itself clearly in the spectroscopic properties of these compounds as already shown by studies on photoexcited singlet and triplet states.[3-5] A comparison of porphycenes and porphyrins, especially from the viewpoint of electronic structure and photochemical reactivity, must also include an inspection of the doublet-state radical ions of porphycenes. In a short communication, first ESR and multiple electron-nuclear resonance characterizations of the free-base porphycene anion radical have been reported.[6a] From independent investigations, electrochemical, ESR, ENDOR, and EXAFS characterizations of a nickel(II) porphycene anion radical have been reported very recently.[6b,c]

In the present publication we report in more detail on ESR, electron-nuclear double resonance (ENDOR), and electron-nuclear-nuclear triple resonance (TRIPLE) measurements of isotropic interaction parameters such as *g*-factors and $^1H$ and $^{14}N$ hyperfine coupling constants (hfc's) of the anion radicals of the following porphycenes (see Figure 1): **1**, unsubstituted free-base porphycene ($H_2PC1$); **2**, 2,7,12,17-tetra-*n*-propylporphycene ($H_2PC2$); **3**, 9,10,19,20-tetra-*n*-propylporphycene ($H_2PC3$); **4**, unsubstituted zinc porphycene (ZnPC1); **5**, 2,7,12,17-tetra-*n*-propylnickel porphycene (NiPC2); **6**, 2,7,12,17-tetra-*n*-propylpalladium porphycene (PdPC2); and **7**, 2,7,12,17-tetra-*n*-propylplatinum porphycene (PtPC2). The spectroscopic results for $H_2PC1^{\bullet-}$, $H_2PC2^{\bullet-}$, and $H_2PC3^{\bullet-}$ are compared with spin density distributions obtained from all-valence-electrons self-consistent field molecular orbital (SCF MO) calculations of the type RHF-INDO/SP.[7]

## Experimental Section

The porphycenes were reduced chemically with sodium metal under high-vacuum conditions.[8] Tetrahydrofuran (THF) dried over a Na/K alloy was used as a solvent. The porphycene concentration was about $5 \times 10^{-4}$ M. The radicals were stable over at least several weeks when stored at −27 °C. The anion radicals of $H_2PC1$ were also generated by potentiostatically controlled electrolysis in THF using tetra-*n*-butyl-

[†] Institut für Molekülphysik, Freie Universität Berlin.
[‡] Institut für Organische Chemie, Freie Universität Berlin. Present address: University of California San Diego, Department of Physics, La Jolla, CA 92093.
[§] The Hebrew University of Jerusalem.
[⊥] Universität Köln.

(1) (a) Vogel, E.; Köcher, M.; Schmickler, H.; Lex, J. *Angew. Chem.* **1986**, *98*, 262; *Angew. Chem., Int. Ed. Engl.* **1986**, *25*, 257. (b) Vogel, E.; Köcher, M.; Lex, J.; Ermer, O. *Isr. J. Chem.* **1989**, *29*, 257.
(2) Köcher, M. Ph.D. Thesis, Universität Köln, West Germany, 1988.
(3) Ofir, H.; Regev, A.; Levanon, H.; Vogel, E.; Köcher, M.; Balci, M. *J. Phys. Chem.* **1987**, *91*, 2686.
(4) Levanon, H.; Toporowicz, M.; Ofir, H.; Fessenden, R. W.; Das, P. K.; Vogel, E.; Köcher, M.; Pramod, K. *J. Phys. Chem.* **1988**, *92*, 2429.
(5) Toporowicz, M.; Ofir, H.; Levanon, H.; Vogel, E.; Köcher, M.; Pramod, K.; Fessenden, R. W. *Photochem. Photobiol.* **1989**, *50*, 37.
(6) (a) Schlüpmann, J.; Huber, M.; Toporowicz, M.; Köcher, M.; Vogel, E.; Levanon, H.; Möbius, K. *J. Am. Chem. Soc.* **1988**, *110*, 8566. (b) Renner, M. W.; Forman, A.; Wu, W.; Chang, C. K.; Fajer, J. *J. Am. Chem. Soc.* **1989**, *111*, 8618. (c) Furenlid, L. R.; Renner, M. W.; Smith, K. M.; Fajer, J. *J. Am. Chem. Soc.* **1990**, *112*, 1634.
(7) Plato, M.; Tränkle, E.; Lubitz, W.; Lendzian, F.; Möbius, K. *Chem. Phys.* **1986**, *107*, 185.
(8) Paul, D. E.; Lipkin, D.; Weissman, S. I. *J. Am. Chem. Soc.* **1956**, *78*, 116.

0002-7863/90/1512-6463$02.50/0 